BULETINUL INSTITUTULUI POLITEHNIC DIN IAȘI
Publicat de
Universitatea Tehnică „Gheorghe Asachi” din Iași
Volumul 65 (69), Numărul 1, 2019
Secția
CONSTRUCȚII DE MAȘINI

A STUDY ABOUT DYNAMICS OF AN INERTIAL TRANSPORT MECHANISM ACTUATED BY A FOUR BAR LINKAGE

BY

EUGEN CORDUNEANU[1] and FLORENTIN BUIUM[2,*]

"Gheorghe Asachi" Technical University of Iași, Romania,
[1]Department of Theoretical Mechanics
[2]Department of Mechanical Engineering, Mechatronics and Robotics

Received: June 3, 2019
Accepted for publication: June 25, 2019

Abstract. The paper presents a practical application of the four bar linkage in the field of inertial transportation. Rectilinear movement of a rigid body on a horizontal plane in an imposed direction is given by inertial force developed by sitting plane movement. Thus, sitting plane is tied to a four bar rocker, horizontal pose being obtained from another four bar linkage (of parallelogram type). Connecting rod of this linkage imposes the circular translation movement of the sitting plane. This complex mechanism may be regarded as composed by two four bar linkages, one of common type and another of parallelogram type, rocker of the first being at the same time, crank of the later. The goal of this study is the rigid body movement on the horizontal plane. Under the circumstance that the driving link is the crank of the four bar linkage, the problem is about relative motion dynamics (of the rigid body on the sitting plane).

Keywords: four bar linkage; parallelogram linkage; circular translation; relative movement.

---

[*]Corresponding author; *e-mail*: fbuium@gmail.com

1. Introduction

The experimental inertial transport mechanism with its kinematic components is shown in Fig. 1. Electric DC engine supplied from a transformer actuates the driving crank, by a worm gear.

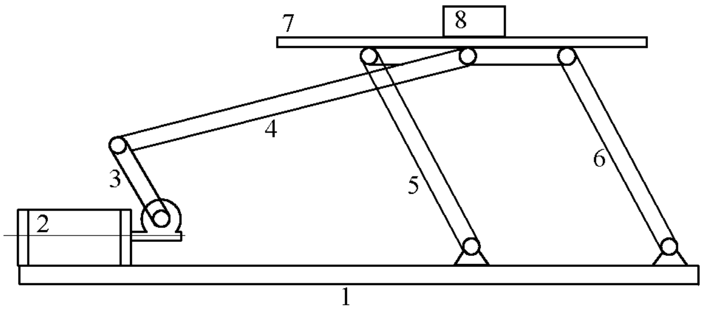

Fig. 1 – The inertial transport mechanism (experimental model): 1 – fixed support, 2 – electric DC engine, 3 – driving crank, 4 – connecting rod, 5 – rocker, 6 – rocker in parallelogram linkage, 7 – sitting plane, 8 – solid body denoted by (*W*).

The four bar linkage is composed by the crank (3), the connecting rod (4), the rocker (5) and the fixed support (1). The parallelogram mechanism is composed by the rockers (5) and 6), the connecting rod (7) and the connecting rod (7) being at the same time the sitting plane on which the solid body moves.

The subject of this study is the motion of the solid body (*W*). The dynamic study represents a problem of relative motion dynamics, that is the rectilinear movement of the body (*W*) on the sitting plane. The circular alternative translation motion of the sitting plane (7) is the transport motion.

As hypothesis there are known the four bar driving constructive characteristics of the mechanism, the angular velocity of the crank and the friction coefficient between body (*W*) and the sitting plane. The (*W*) body is supposed of rectangular shape.

2. Constructive and Initial Considerations

The mechanism dynamical study requires two stages. In the first one the parameters of the rocker transport motion are determined, this being a problem of kinematics. In the second the relative motion of (*W*) body is studied, this being problem of dynamics (Duca *et al*., 2003).

A mechanical model of the four bar linkage driving mechanism it is considered (Fig. 2). In this diagram, the following notations are made (as in the figure): *O* – the crank revolute pair, C – the rocker revolute pair, *A*, *B* – the connecting rod pairs, d_0 - the horizontal length between *O* and *C*, *h* – the vertical length between *O* and *C*. We also denote by r – the crank radius, b – the rocker length and l – the connecting rod length.

The mechanical model is reported to an orthogonal system Oxy having the Ox axis collinear with the direction of the fixed pairs (O,C).

The constructive parameters of the driving mechanism are the lengths of the crank, of the connecting rod, of the rocker and the length of the distance between the fixed pairs (O,C). These lengths and their notation, accorded with Fig. 2, are presented in Table 1.

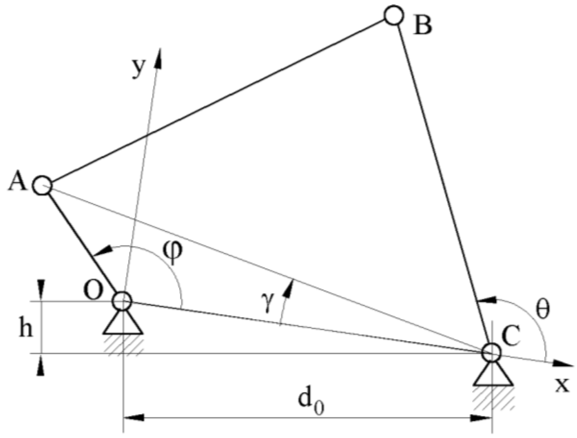

Fig. 2 – The scheme of the driving four bar mechanism.

Knowing d_0 = 38 cm and h = 3 cm, the length between *O* and *C* fixed joints can be calculated:

$$d = \sqrt{d_0^2 + h^2} = \sqrt{38^2 + 3^2} = 38.12 \text{ cm}. \quad (1)$$

Table 1
The Lengths of the Elements

Link	Notation		Length [cm]
	Fig. 1	Fig. 2	
Crank	3	*OA*	$r = 6$
Connecting rod	4	*AB*	$l = 50$
Rocker	5	*CB*	$b = 30$
Fixed support	1	*OC*	$d = 38.12$

The angles in Fig. 2 have following significance: φ – the crank position angle $\varphi = \sphericalangle\,(OX,\ OA)$ ccw., θ – the rocker position angle, $\theta = \sphericalangle\,(OX,\ CB)$ ccw., γ – the angle between *OX* axis and *CA* variable line, $\gamma = \sphericalangle(OX, CA)$ cw.

3. Driving Mechanism Kinematics

The 1st stage of the study consists in solving the four bar linkage kinematics. Thus, it is determined the rocker angle γ as function of the crank angle φ. Knowing the crank motion law, the rocker kinematical parameters are determined.

Applying Pythagoras Generalized Theorem in the ΔABC (Fig. 2), the following relationship can be written (Rogai and Teodorescu, 1975):

$$\cos(\theta+\gamma)=\frac{l^2-b^2-f^2}{2bf}, \tag{2}$$

where $f=AC$, variable length.

Applying the same theorem in the ΔAOC (Fig. 2), it results:

$$f^2=r^2+d^2-2r\cdot d\cdot\cos\varphi,\quad d=OC,$$

$$f(\varphi)=\sqrt{r^2+d^2-2r\cdot d\cdot\cos\varphi}. \tag{3}$$

From the ΔAOC, the following relations can be expressed (Rogai and Teodorescu, 1975):

$$\tan\gamma=\frac{r\cdot\sin\varphi}{d-r\cdot\cos\varphi}, \tag{4}$$

$$\sin\gamma=\frac{r\cdot\sin\varphi}{f},\quad \cos\gamma=\frac{d-r\cdot\cos\varphi}{f}. \tag{5}$$

The Eq. (4) and the Eq. (5) appear more clear if in Fig. 2, an auxiliary construction is made by projecting the point A on OX axis: $AA_0\perp OX$, $A_0\in OX$.

By introducing the constant positive value

$$a^2=l^2-b^2, \tag{6}$$

Eq. (2) can be written

$$\theta+\gamma=\arccos\frac{a^2-f^2}{2b\cdot f}, \tag{7}$$

And by replacing γ according to Eq. (4) it results:

$$\theta = \arccos \frac{a^2 - f^2}{2b \cdot f} - \arctan \frac{r \cdot \sin \varphi}{d - r \cdot \cos \varphi}, \tag{8}$$

where f is given by Eq. (3).

Eq. (8) shows the function $\theta = \theta(\varphi)$, that is the output position parameter as function of input independent variable of the driving four bar linkage.

For kinematic purpose it admits that crank performs a uniform rotation ccw. motion, expressed by the relationship

$$\varphi(t) = \omega_0 t, \ t \geq 0, \tag{9}$$

where ω_0 is a constant angular velocity and t denotes the time.

By performing the derivative of Eq. (7) with respect to time, it results:

$$\dot{\theta} + \dot{\gamma} = \frac{a^2 + f^2}{\sqrt{4b^2 f^2 - \left(a^2 - f^2\right)^2}} \cdot \frac{\dot{f}}{f}, \tag{10}$$

where $\dot{\theta} = \dfrac{d\theta}{dt}$, $\dot{\gamma} = \dfrac{d\gamma}{dt}$, $\dot{f} = \dfrac{df}{dt}$.

Calculating the derivative of the function f accordingly to the Eq. (3), it obtains:

$$\dot{f} = \omega_0 r \cdot d \frac{\sin \varphi}{f}, \tag{11}$$

By replacing Eq. (11) in Eq. (10) it results:

$$\dot{\theta} = \frac{\omega_0 r \cdot d \left(a^2 + f^2\right) \sin \varphi}{f^2 \sqrt{4b^2 f^2 - \left(a^2 - f^2\right)^2}} - \dot{\gamma}, \tag{12}$$

By computing the derivative of Eq. (4) with respect the time it obtains:

$$\frac{\dot{\gamma}}{\cos^2 \gamma} = \frac{\omega_0 r \cos \varphi \left(d - r \cos \varphi\right) - r \sin \varphi \left(\omega_0 r \sin \varphi\right)}{\left(d - r \cos \varphi\right)^2},$$

or still,

$$\dot{\gamma}\left(1 + \tan^2 \gamma\right) = \frac{\omega_0 r \cdot d \cos \varphi - \omega_0 r^2}{\left(d - r \cos \varphi\right)^2}, \tag{13}$$

Based on Eq. (4) it results the following equation

$$1+\tan^2\gamma = 1+\frac{r\sin^2\varphi}{\left(d-r\cos\varphi\right)^2} = \frac{f^2}{\left(d-r\cos\varphi\right)^2}\,, \tag{14}$$

where f was replaced according to Eq. (3).

Replacing Eq. (14) in Eq. (13), it results:

$$\dot{\gamma} = \omega_0 r\cdot\frac{d\cos\varphi - r}{f^2}\,, \tag{15}$$

By substituting Eq. (15) in Eq. (12), the rocker angular velocity it is obtained:

$$\omega = \dot{\theta} = \frac{\omega_0 r}{f^2}\left[\frac{d\left(a^2+f^2\right)\sin\varphi}{\sqrt{4b^2 f^2-\left(a^2-f^2\right)^2}} + r - d\cos\varphi\right], \tag{16}$$

where f is given by Eq. (3) and φ is given by Eq. (9): $f(\varphi) = \sqrt{r^2+d^2-2r\cdot d\cdot\cos\varphi}$, $\varphi(t) = \omega_0 t$ where f is a composed function of time by angle φ.

The derivative of Eq. (10) with respect the time is:

$$\ddot{\theta}+\ddot{\gamma} = \frac{\ddot{f}\cdot f\left(f^2+a^2\right)+\dot{f}^2\left(f^2-a^2\right)}{f^2\sqrt{4b^2f^2-\left(a^2-f^2\right)^2}} + \frac{2\dot{f}^2\left(f^2+a^2\right)\left(f^2-2b^2-a^2\right)}{\left(\sqrt{4b^2f^2-\left(a^2-f^2\right)^2}\right)^3} \tag{17}$$

where $\ddot{\theta} = \frac{d^2\theta}{dt^2}$, $\ddot{\gamma} = \frac{d^2\gamma}{dt^2}$, $\ddot{f} = \frac{d^2 f}{dt^2}$.

Calculating the derivative of second order of function f with respect the time, according to Eq. (11), it obtains

$$\ddot{f} = \omega_0 r\cdot d\,\frac{\omega_0 f\cos\varphi - \dot{f}\sin\varphi}{f^2}\,, \tag{18}$$

where, after $\dot{f}$ is substituted according to Eq. (11), it results:

$$\ddot{f} = \omega_0 r\cdot d\,\frac{\omega_0 f\cos\varphi - \omega_0 r\cdot d\cdot\sin\varphi}{f^2}\,,$$

and yet

$$\ddot{f} = \frac{\omega_0^2 r\cdot d}{f^3}\left(f^2\cos\varphi - r\cdot d\cdot\sin^2\varphi\right). \tag{19}$$

Calculating the second order derivative of the angle γ according to Eq. (15), it obtains,

$$\ddot{\gamma} = \frac{\omega_0 r}{f^4}\left[\omega_0 d \cdot f^2 \sin\varphi + 2f \cdot \dot{f}\left(d\cos\varphi - r\right)\right], \tag{20}$$

relationship where $\dot{f}$ is substituted according to the Eq. (11) and it results:

$$\ddot{\gamma} = \frac{\omega_0 r \cdot d}{f^4}\left(2r^2 \sin\varphi - r \cdot d \cdot \sin 2\varphi - f^2 \sin\varphi\right). \tag{21}$$

After replacing Eq. (21) in Eq. (17), the rocker angular acceleration is obtained:

$$\varepsilon = \ddot{\theta} = \frac{\ddot{f} \cdot f\left(f^2 + a^2\right) + \dot{f}^2\left(f^2 - a^2\right)}{f^2\sqrt{4b^2 f^2 - \left(a^2 - f^2\right)^2}} + \frac{2\dot{f}^2\left(f^2 + a^2\right)\left(f^2 - 2b^2 - a^2\right)}{\left(\sqrt{4b^2 f^2 - \left(a^2 - f^2\right)^2}\right)^3} + \frac{\omega_0 r \cdot d \sin\varphi}{f^4}\left(f^2 + 2r \cdot d \cdot \cos\varphi - 2r^2\right), \tag{22}$$

where f is given in Eq. (3) and φ in Eq. (9)

$$f(\varphi) = \sqrt{r^2 + d^2 - 2r \cdot d \cdot \cos\varphi}, \; \varphi(t) = \omega_0 t,$$

and $\dot{f}$ is given in Eq. (11) and $\ddot{f}$ in Eq. (19)

$$\dot{f} = \omega_0 r \cdot d\,\frac{\sin\varphi}{f}, \; \ddot{f} = \frac{\omega_0^2 r \cdot d}{f^3}\left(f^2 \cos\varphi - r \cdot d \cdot \sin^2\varphi\right),$$

where f, $\dot{f}$ and $\ddot{f}$ are composed functions of time through φ.

As conclusions of the performed kinematical study, the followings can be noticed:

1. The constructive parameters of driving four bar linkage were considered input data: *r*, *l*, *b*, *d* (Fig. 2). The constant angular velocity ω_0 is supposed to be known;

2. The angular position of the rocker as function of time given by relationship (8) is obtained:

$$\theta\left(t\right) = \arccos\frac{a^2 - f^2}{2b \cdot f} - \arctan\frac{r \cdot \sin\varphi}{d - r \cdot \cos\varphi}; \tag{23}$$

3. The rocker angular velocity given by the derivative of the first order of the function $\theta\left(t\right)$ with respect the time, given by Eq. (16), is obtained

$$\omega(t)=\frac{\omega_0 r}{f^2}\left[\frac{d\left(a^2+f^2\right)\sin\varphi}{\sqrt{4b^2 f^2-\left(a^2-f^2\right)^2}}+r-d\cos\varphi\right]; \tag{24}$$

4. The rocker angular acceleration given by the derivative of the second order of the function $\theta(t)$ with respect the time, given by Eq. (22), is obtained:

$$\varepsilon(t)=\frac{\ddot{f}\cdot f\left(f^2+a^2\right)+\dot{f}^2\left(f^2-a^2\right)}{f^2\sqrt{4b^2 f^2-\left(a^2-f^2\right)^2}}+\frac{2\dot{f}^2\left(f^2+a^2\right)\left(f^2-2b^2-a^2\right)}{\left(\sqrt{4b^2 f^2-\left(a^2-f^2\right)^2}\right)^3}+$$
$$+\frac{\omega_0 r\cdot d\sin\varphi}{f^4}\left(f^2+2r\cdot d\cos\varphi-2r^2\right), \tag{25}$$

Eq. (23), Eq. (24) and Eq. (25) are implicit periodical functions of time, with the period $T=2\pi/\omega_0$.

In Eq. (23) and Eq, (24) are used the notations given by Eq. (3), Eq. (6) and Eq. (9):

$$f(\varphi)=\sqrt{r^2+d^2-2rd\cdot\cos\varphi},\ a^2=l^2-b^2,\ \varphi(t)=\omega_0 t \tag{26}$$

In Eq. (25) are used the same notations and also the derivative of the 1st and the 2nd order of the function f with respect the time, given by Eq. (11) and Eq. (19):

$$\dot{f}=\omega_0 r\cdot d\frac{\sin\varphi}{f},\quad \ddot{f}=\frac{\omega_0^2 r\cdot d}{f^3}\left(f^2\cos\varphi-r\cdot d\cdot\sin^2\varphi\right) \tag{27}$$

4. Dynamical Study

In the 2nd stage of this paper, the dynamical study of the parallelogram mechanism was made. It consists in calculus of the body (*W*) displacement on the sitting plane, considering as hypothesis all the results of the kinematical study, obtained in the previous paragraph.

The dynamical study represents a problem of relative motion dynamics. The rectilinear movement of the body (*W*) on the sitting plane is a relative one. The translation circular alternative motion of sitting plane is a transport motion. The body (*W*) motion reported to the fixed referential system Oxy (the referential system of the four bar driving linkage) is an absolute motion.

Let us consider an experimental model of the inertial transport mechanism, presented in Fig. 1. The mechanical model represented in Fig. 2 is completed with a parallelogram mechanism, so that crank of this mechanism is, at the same time, the rocker of the previous presented four bar linkage. The parallelogram mechanism, with the connecting rod in the horizontal position, reports to an orthogonal mobile referential system $Bx'y'$ with origin in B and Bx' axis, horizontal, on sitting plane direction (Fig. 3).

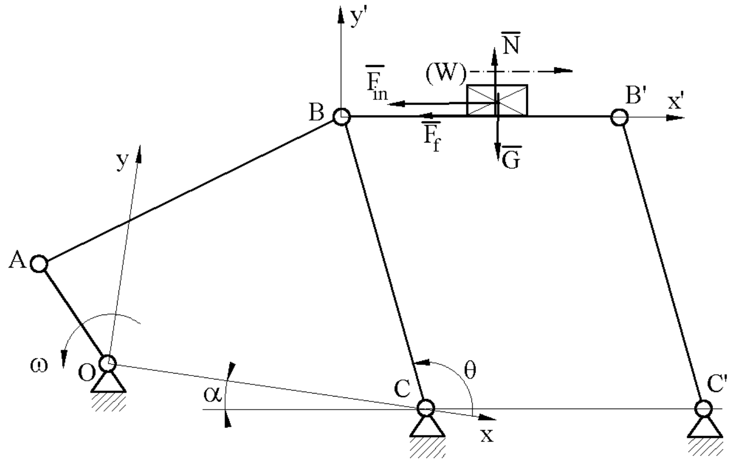

Fig. 3 – The mechanical model of the transport mechanism.

With α is denoted the constant angle between Ox and Bx' axes. According to Fig. 2 and Fig. 3,

$$\alpha = \arctan\frac{h}{d_0} = \arctan\frac{3}{38} \approx 4^\circ 30', \tag{28}$$

with d_0 and h given by Eq. (1).

Taking down m as the body (W) mass, the dynamic equation of its relative motion on the sitting plane is (Mangeron and Irimiciuc, 1978; Teodorescu, 1984):

$$m\bar{a}_r = \bar{G} + \bar{N} + \bar{F}_f + \bar{F}_{in}, \tag{29}$$

where $\bar{a}_r$ is the relative acceleration and the other notations represent the following forces: the gravity force $(\bar{G})$ and the normal reaction $(\bar{N})$ which have vertical direction, the friction force $(\bar{F}_f)$ and the inertial force $(\bar{F}_{in})$ which have horizontal direction (Fig. 3). The friction force has opposite sense to the relative motion and the inertial force has opposite sense to the transport acceleration.

If the body (*W*) coordinate with respect to the mobile system is denoted by x' and if $\overline{i'}$ and $\overline{j'}$ denote the axes unit vectors, the following relationships can be written:

$$\overline{G} = m\overline{g} = -mg \cdot \overline{j'} \text{ and } \overline{N} = N \cdot \overline{j'}, \tag{30}$$

where $\overline{g}$ is gravitational acceleration, g = 9.8 m/s^2;

$$\overline{F}_f = -\mu N\left(\operatorname{sgn} \dot{x}'\right)\overline{i'}, \quad \dot{x}' = \frac{dx'}{dt}, \tag{31}$$

where μ is sliding friction coefficient and 'sgn' is the signum function *i.e*.

$$\overline{F}_f = \begin{cases} -\mu N, \dot{x}' > 0 \\ \mu N, \dot{x}' < 0, \end{cases}$$

$$\overline{a}_r = \ddot{x}'\overline{i'}, \quad \ddot{x}' = \frac{d^2x'}{dt^2}. \tag{32}$$

We note the coordinates of the point *B* with respect to the fixed referential system by *x* and *y* and the axes unit vectors of the same frame by $\overline{i}$ and $\overline{j}$. The transport force of inertia is now:

$$\overline{F}_{in} = -m\overline{a}_t = -m\left(\ddot{x} \cdot \overline{i} + \ddot{y} \cdot \overline{j}\right), \tag{33}$$

where $\overline{a}_t$ is the transport acceleration. The coordinates of the point *B* are obtained according to Fig. 3, where $OC = d$ and $CB = b$:

$$x = d + b \cdot \cos\theta, \quad y = b \cdot \sin\theta, \tag{34}$$

which are composed functions of time, by angle θ.

The velocity components are the derivatives with respect to time of Eq. (34) are

$$\dot{x} = -b \cdot \dot{\theta}\sin\theta, \quad \dot{y} = b \cdot \dot{\theta}\cos\theta, \tag{35}$$

and the components of the acceleration are

$$\begin{aligned} \ddot{x} &= -b \cdot \ddot{\theta}\sin\theta - b \cdot \dot{\theta}^2\cos\theta, \\ \ddot{y} &= b \cdot \ddot{\theta}\cos\theta - b \cdot \dot{\theta}^2\sin\theta. \end{aligned} \tag{36}$$

By using the notations from the previous paragraph, it writes

$$\begin{aligned} \ddot{x} &= -b \cdot \varepsilon \cdot \sin\theta - b \cdot \omega^2 \cos\theta \\ \ddot{y} &= b \cdot \varepsilon \cdot \cos\theta - b \cdot \omega^2 \sin\theta, \end{aligned} \tag{37}$$

θ, ω and ε being determined functions.

Substituting Eq. (30), Eq. (31), Eq. (32) and Eq. (33) in Eq. (29), it obtains

$$m \cdot \ddot{x}' \cdot \overline{i'} = -mg \cdot \overline{j'} + N \cdot \overline{j'} - \mu N \left(\operatorname{sgn} \dot{x}'\right) \overline{i'} - m\left(\ddot{x} \cdot \overline{i} + \ddot{y} \cdot \overline{j}\right), \tag{38}$$

or still,

$$\left[m \cdot \ddot{x}' + \mu N \left(\operatorname{sgn} \dot{x}'\right)\right] \overline{i'} + \left(mg - N\right) \overline{j'} = -m\left(\ddot{x} \cdot \overline{i} + \ddot{y} \cdot \overline{j}\right). \tag{39}$$

The following scalar equation system by performing the scalar vector product between Eq. (39) and the mobile unit vectors $\overline{i'}$ and $\overline{j'}$ results (Mangeron and Irimiciuc, 1978; Teodorescu, 1984):

$$\begin{cases} m \cdot \ddot{x}' + \mu N \left(\operatorname{sgn} \dot{x}'\right) = -m \cdot \ddot{x} \cos\alpha - m \cdot \ddot{y} \sin\alpha \\ mg - N = m \cdot \ddot{x} \sin\alpha - m \cdot \ddot{y} \cos\alpha \end{cases}, \tag{40}$$

By reducing the normal reaction force from Eq. (40), the following equation is obtained

$$\ddot{x}' + \mu\left(g - \ddot{x}\sin\alpha + \ddot{y}\cos\alpha\right)\left(\operatorname{sgn} \dot{x}'\right) = -\ddot{x}\cos\alpha - \ddot{y}\sin\alpha. \tag{41}$$

After replacing Eq. (37) in Eq. (41), it obtains:

$$\begin{aligned} &\ddot{x}' + \mu\left[g + b \cdot \varepsilon \cdot \cos\left(\theta - \alpha\right) - b \cdot \omega^2 \sin\left(\theta - \alpha\right)\right]\left(\operatorname{sgn} \dot{x}'\right) = \\ &= b \cdot \varepsilon \cdot \sin\left(\theta - \alpha\right) + b \cdot \omega^2 \cos\left(\theta - \alpha\right), \end{aligned} \tag{42}$$

that is the differential equation of the relative motion.

In Eq. (42) the angle θ, the angular velocity ω and the angular acceleration ε are previously established as implicit functions of time. Angle θ is given by Eq. (23), angular velocity ω is given by Eq. (24) and angular acceleration ε is given by Eq. (25).

The relative velocity of the body (W), denoted by v, is defined as the derivative with respect to time of the relative coordinate:

$$v = \dot{x}' = \frac{dx'}{dt}, \quad \dot{v} = \ddot{x}' = \frac{d^2 x'}{dt^2}. \tag{43}$$

The initial conditions of motion are:

$$x'(0)=0\,,\;\; v(0)=\dot{x}'(0)=0\,, \tag{44}$$

by supposing that at the initial moment, the body (*W*) is at rest in *B* position.

In order to numerically solve the differential Eq. (42) with the initial conditions given by Eq. (44), it is used a computer aided numerical procedure. According to Eq. (43), the differential equation given by Eq. (42) is written in the equivalent form of a system of two differential equations of the first order:

$$\begin{cases} \dot{x}'(t)=v(t) \\ v=\mu\left[b\cdot\omega^2\sin(\theta-\alpha)-b\cdot\varepsilon\cos(\theta-\alpha)-g\right]\operatorname{sgn}v+ \\ +b\cdot\varepsilon\sin(\theta-\alpha)+b\cdot\omega^2\cos(\theta-\alpha). \end{cases} \tag{45}$$

The Eq. (45) with initial conditions given by Eq. (44) is numerically integrated by using a procedure of the following type:

$$Odesolve\left(\begin{pmatrix} x' \\ v \end{pmatrix},t,t_f,p_0\right),t\in\left[0,t_f\right], \tag{46}$$

where t_f is the final moment of time interval inside which the motion is studied and p_0 is the number of points (time moments) for which solution is given.

By numerical integration of system (45) the relative coordinate (displacement) and the relative velocity are obtained as functions of time

$$x'=x'(t)\,,\;\; v=v(t)\,,\; t\in\left[0,t_f\right], \tag{47}$$

these being the conclusions of the performed dynamical study.

The angular velocity of the driving crank with respect to the number of rotations per minute $n_0=100\langle rpm\rangle$, is

$$\omega_0=\frac{\pi n}{30}=10.466\ \text{s}^{-1}. \tag{48}$$

According to Eq. (48), the time period of the transport motion is

$$T=\frac{2\pi}{\omega_0}\simeq 0.6\ \text{s} \tag{49}$$

The numerical values are of the input data are given in Table 1 and by Eq. (1), Eq. (28) and Eq. (48):

$$r=6\ \text{cm}\,,\;\; l=50\ \text{cm}\,,\; b=30\ \text{cm}\,,\; d=38.12\ \text{cm}\,,\; \alpha=4^{\text{o}}30'\,, \\ \omega_0=10.466\ \text{s}^{-1}\,, \tag{50}$$

to which the gravitational acceleration g = 9.8 m/s^2 is added.

In Fig. 4 is shown the function $\theta = \theta(\varphi)$ given by Eq. 8.

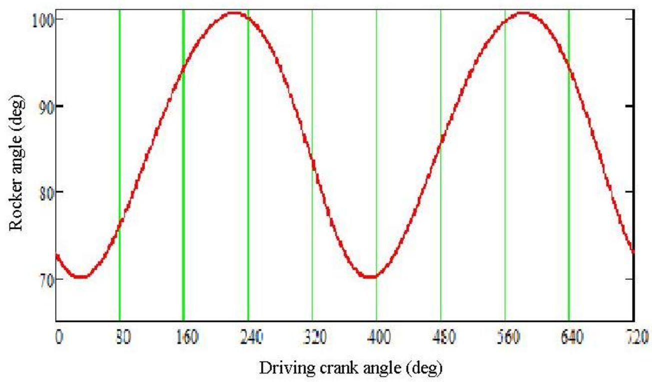

Fig. 4 – Rocker angle θ *versus* crank angle φ.

In Fig. 5 to Fig. 13 are presented the numerical results obtained by solving the differential equation system given by Eq. (45) with initial conditions given by Eq. (44), that is the displacement diagrams $x'(t)$ and velocity diagrams $v(t)$ as functions of time, for different friction coefficient values.

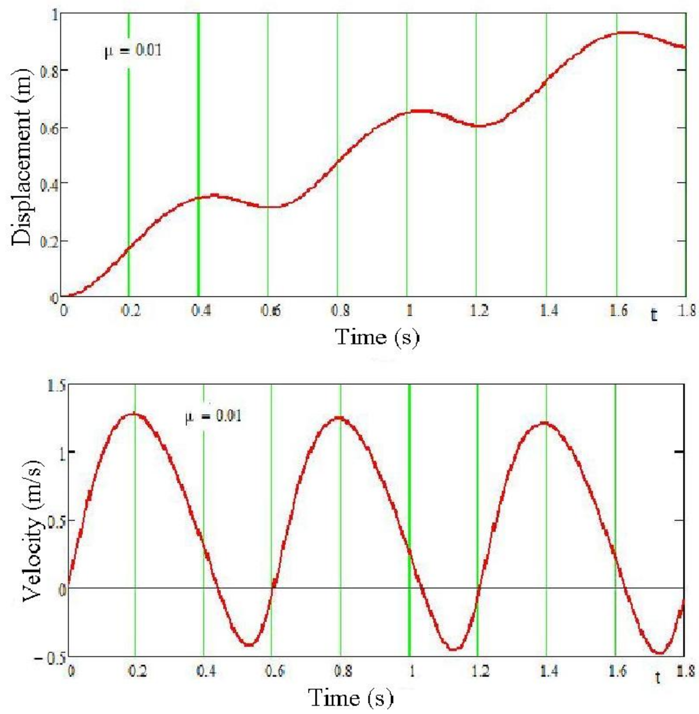

Fig. 5 – Diagrams of displacement and velocity for $\mu = 0.01$.

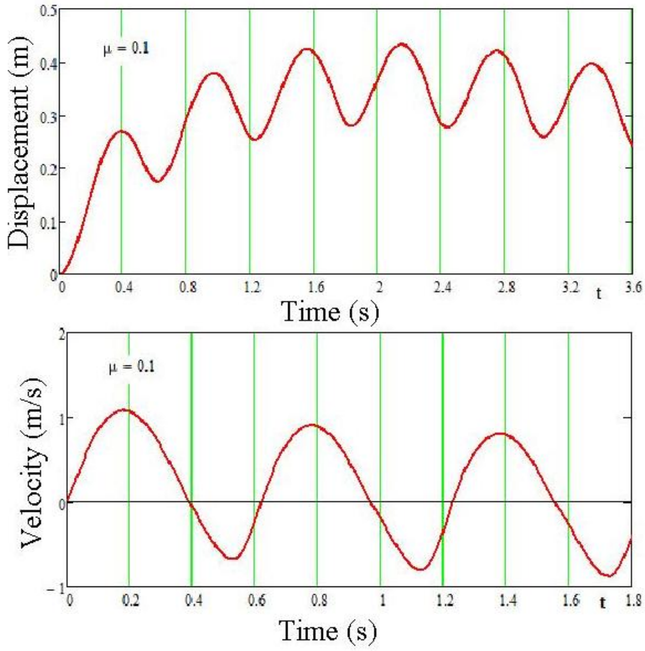

Fig. 6 – Diagrams of displacement and velocity for $\mu = 0.1$.

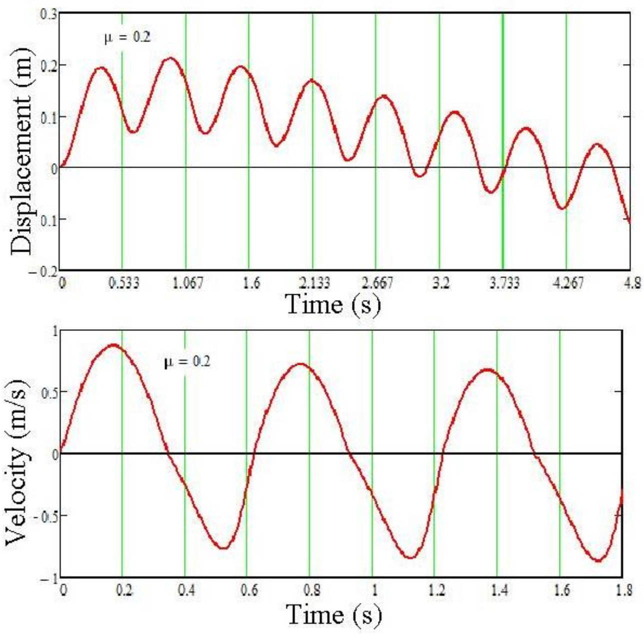

Fig. 7 – Diagrams of displacement and velocity for $\mu = 0.2$.

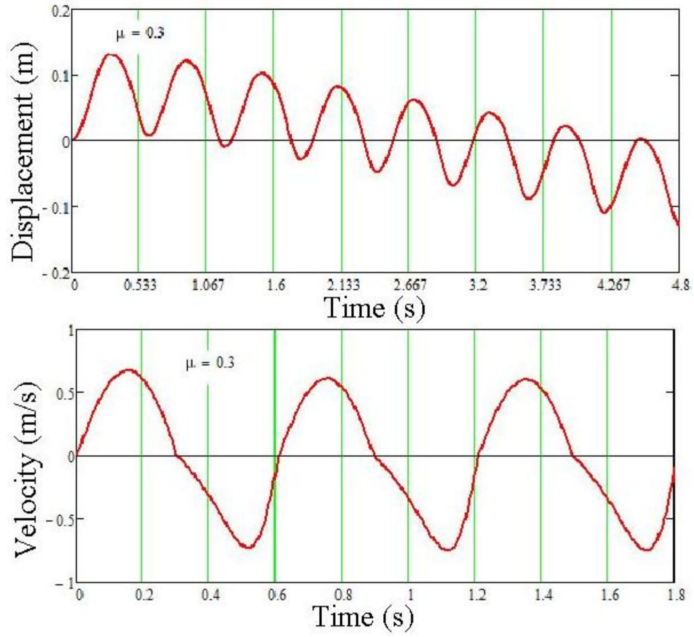

Fig. 8 – Diagrams of displacement and velocity for $\mu = 0.3$.

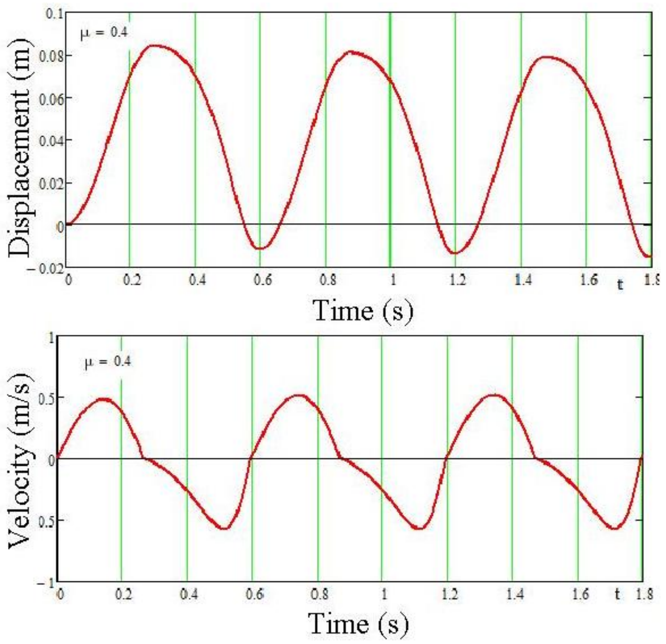

Fig. 9 – Diagrams of displacement and velocity for $\mu = 0.4$.

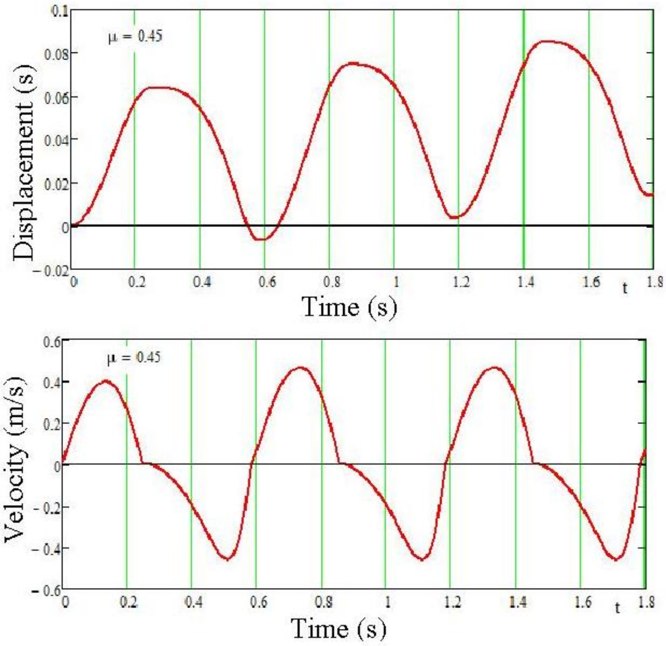

Fig. 10 – Diagrams of displacement and velocity for $\mu = 0.45$.

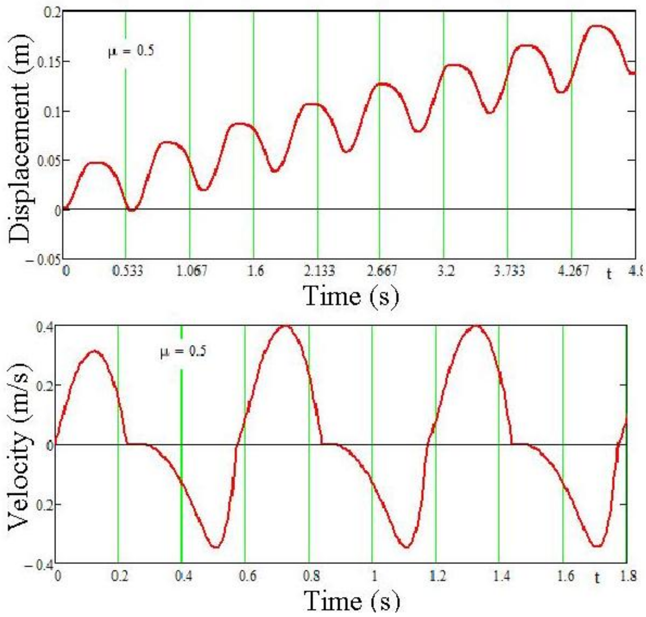

Fig. 11 – Diagrams of displacement and velocity for $\mu = 0.5$.

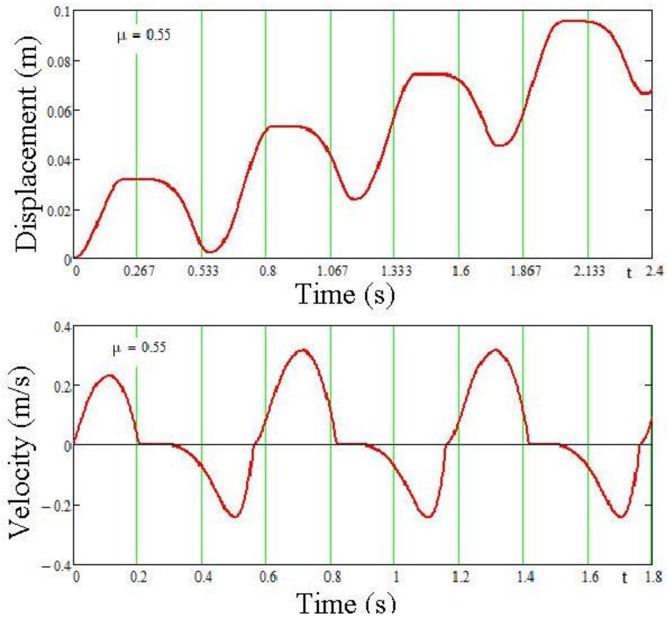

Fig. 12 – Diagrams of displacement and velocity for $\mu = 0.55$.

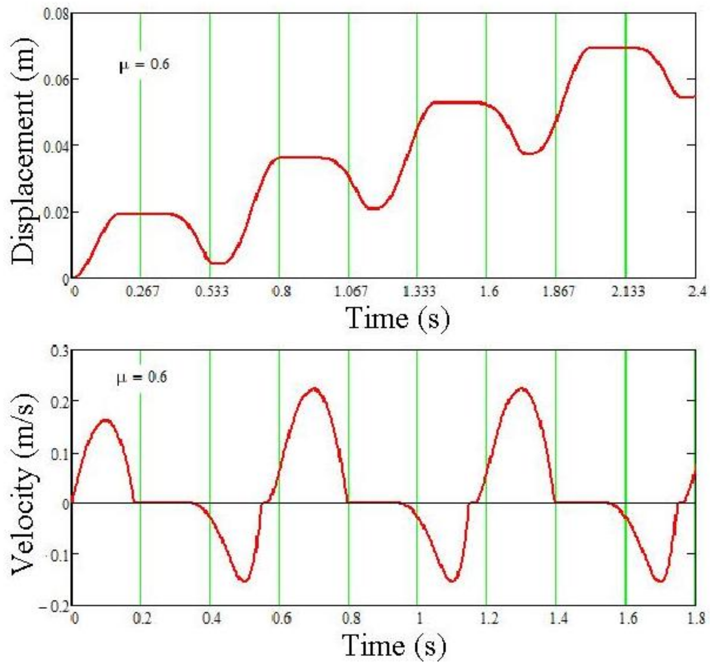

Fig. 13 – Diagrams of displacement and velocity for $\mu = 0.6$.

4. Conclusions

1) Graphical results show that relative motion of (*W*) body on the sitting plane is a pseudo periodical one, having approximative the same period as the transport motion, given by Eq. (49).

2) The extreme points of $v(t)$ functions appear on the diagram at approximately the same value. The extreme points of the $x'(t)$ functions are increasing or decreasing depending on the friction coefficient value.

3) If $x'(t)$ function extremes are increasing, then (*W*) body motion occurs to the right side, in the positive axis direction.

4) If $x'(t)$ function extremes are decreasing, then (*W*) body motion occurs to the left side, in the negative axis direction.

5) The displacement direction of the (*W*) body depends on the numerical value of the friction coefficient. When the friction coefficient is very small (0.01) or very high (0.45 or greater) the motion of the (*W*) body is to the right side. When the friction coefficient is medium (0.1-0.4) the motion of the (*W*) body is to the left side.

REFERENCES

Duca C., Buium Fl., Pârăoaru G., *Mecanisme*, Ed. "Gh. Asachi" Iaşi, 2003.

Mangeron D., Irimiciuc N., *Mechanics of Rigid Bodies with Application in Engineering Vol. I - Mechanics of Rigid Body* (in Romanian), Technical Ed. Bucharest (1978).

Rogai I., Teodorescu C., *Usual Mathematical Tables* (in Romanian), (8^{th} Revised and Improved Edition), Technical Ed. Bucharest (1975).

Teodorescu P.P., *Mechanical Systems. Classical Models Vol. I*, (in Romanian), Technical Ed. Bucharest (1984).

STUDIUL DINAMIC AL UNUI SISTEM MECANIC DE TRANSPORT INERŢIAL ACŢIONAT PRIN MECANISM PATRULATER

(Rezumat)

Lucrarea prezintă o analiză cinematică şi dinamică a unui mecanism de clasa 3, ordin 3, care poate fi tratat ca un mecanism complex format prin înserierea a două mecanisme patrulatere din care unul este paralelogram. Pentru derularea studiului s-au folosit parametri constructivi caracteristici unui model experimental existent. Ca rezultat al integrării numerice a ecuaţiei de mişcare s-au obţinut diferite diagrame cinematice specifice unor valori ale coeficientului de frecare dintre rigidul a cărui mişcare o studiem şi suprafaţa de reazem.